First-principles study of structural, electronic and magnetic properties of diluted magnetic semiconductor and superlattice based on Cr-doped ZnS and ZnSe compounds in wurtzite-type crystal

M. Hadj Zoubir[a], O. Cheref[a,b], M. Merabet[a,b], S. Benalia[a,b], L. Djoudi[a,b], D. Rached[a], and M. Boucharef[a,b]

[a]*Magnetic Materials Laboratory, Faculty of Exact Sciences, Djillali Liabes University of Sidi Bel Abbes, 22000, Sidi Bel-Abbes, Algeria*

[b]*Modelling and Simulation of Magnetic Properties of Heterostructures Laboratory, Faculty of Sciences and Technology, Tissemsilt University, Algeria*

Received 30 July 2022; accepted 9 July 2022

We performed first-principle calculations to investigate the structural, electronic, and magnetic properties of ZnS and ZnSe binary compounds, Zn_5Cr_5S and Zn_5Cr_5Se DMS alloys and $(ZnS)_2/Zn_5Cr_5Se$ and $(ZnSe)_2/Zn_5Cr_5S$ superlattices in the wurtzite structure using the full potential linear muffin-tin orbital (FP-LMTO) method. Features such as lattice constant, modulus of compressibility and its first derivative, spin-polarized band structures, total and local or partial electronic densities of states and magnetic properties were calculated. The electronic structure shows that Zn_5Cr_5S and Zn_5Cr_5Se DMS alloys and $(ZnS)_2/Zn_5Cr_5Se$ and $(ZnSe)_2/Zn_5Cr_5S$ superlattices are half-metallic ferromagnetic with 100% complete spin polarization. The total magnetic moments calculated show the same integer value of 4 μB, which confirms the ferromagnetic half-metallic behavior of these compounds. We found that the ferromagnetic state is stabilized by the p-d exchange associated with the double-exchange mechanism. Zn_5Cr_5S and Zn_5Cr_5Se DMS alloys and $(ZnSe)_2/Zn_5Cr_5Se$ and $(ZnSe)_2/Zn_5Cr_5S$ superlattices are shown to be promising new candidates for applications in the fields of spintronics.

Keywords: FP-LMTO; DMS; superlattices; spintronics.

DOI: https://doi.org/10.31349/RevMexFis.70.020501

1. Introduction

Until now, in the devices marketed within our computers and mobile phones, for example, there are two distinct structures. On the one hand, devices based on diamagnetic semiconductors, which ensure the processing and passage of information [1,2]. These devices use the charge properties of electrons (or holes) to control the flow of current through the circuit. On the other hand, devices based on ferromagnetic metals, which store information, [3,4]. These devices rely on another fundamental property of mater: the global behavior of electron spins. The considerable improvement in the performance of these electronic and magnetic devices increasingly requires miniaturization down to nanometric dimensions. At these dimensions, where certain quantum phenomena appear, technological and fundamental obstacles slow down the practical realization of new materials. It is in this sense that spintronics [5,6], or spin electronics, is arousing great interest in the scientific community as an alternative to classical electronics. Spintronics proposes to use the charge and the spin of the electron together to encode information. This opens up exciting new perspectives in integrability, switching speed, consumption and non-volatility of information [7,8]. The recent demonstration of ferromagnetism in diluted magnetic semiconductors (DMS) [9-11] has shown that DMS is a source of spin compatible with existing semiconductor technology. Therefore, such a material would make it possible to process both the transport and the storage of information thanks to a single building block. DMS has gained much attention as materials for spintronic applications [12-17] due to their half-metallic ferromagnetic (HMF) behavior at Curie temperatures above room temperature [18-20]. The promising ferromagnetic properties of DMS have been verified theoretically and even experimentally for many alloys such as ZnCrSe [21,22], ZnCrS [23], ZnCrTe [24], CdCrS [25], Cd_xCr_{1-x}(S,Se,Te) [26] and Zn_xCr_{1-x}(S, Se, Te) [27]. In another chapter, two-dimensional heterostructures, in which charge carriers are strongly confined in one direction, are the subject of highly deep research activities [28-30]. The most widespread are the superlattices, which are composed of an alternating assembly of semiconducting materials thin layers, their thickness and compositions could be adjusted according to the desired electronic or optical properties. Superlattices have already been used in a gigantic number of devices including high mobility transistors [31], light emitting diodes [32] or laser diodes [33,34]. In addition, superlattices have recently drawn attention for potential applications as thermoelectric materials due to their possible electron confinement effects, and their suppressed thermal conductivity [35-37]. While the superlattices and DMS separately spawned two of the fastest technologies of our time, little has been done to combine the two to function simultaneously in the same material, an idea that may lead to further improvements in information technology, beyond the limits of miniaturization. The injection of magnetic impurity into one of the layers forming the superlattice, gives a heterostructure possessing magnetic properties which is the aim of this work. DMS heterostructures or DMS based superlattices offer many unique

opportunities for the study of spin dependent effects. The possible formation of spin superlattices was suggested by von Ortenberg [38] who proposed the concept of a spin superlattice consisting of alternating layers of semimagnetic and nonmagnetic semiconductors. The formation of spin superlattices has been demonstrated in ZnSe/$Zn_{1-x}Fe_xSe$ [39,40], ZnSe/$Zn_{1-x}Mn_xSe$ [41,42], and later in CdTe/$Cd_{1-x}Mn_xTe$ [43,44], $Zn_{1-x}Mn_xSe$/$Zn_{1-y}Fe_ySe$ [45], and $Cd_{1-x}Mn_xTe$/$Cd_{1-y}Mg_yTe$ [46]. The major challenge is therefore to manage to develop superlattices as close as possible to the two-dimensional heterostructures of microelectronics but which also exhibit magnetic properties strongly coupled to electronic properties. This would extend the advantages of spin electronics and the possibilities of microelectronics. DMS based superlattices offer several parameters which can be controlled and modified according to technological needs (n-type or p-type doping, magnetic dopants, thickness and compositions). In this paper we studied the structural, electronic, and magnetic properties of the ZnS and ZnSe binary compounds, $Zn_{0.5}Cr_{0.5}S$ and $Zn_{0.5}Cr_{0.5}Se$ DMS alloys and $(ZnS)_2$/$Zn_{0.5}Cr_{0.5}Se$ and $(ZnSe)_2$/$Zn_{0.5}Cr_{0.5}S$ DMSs based quantum well superlattices in the framework of the density functional theory (DFT). This paper is organized as follows. In Sec. 2, the calculation method is presented. In Sec. 3, the numerical results are shown and discussed. Finally, a brief conclusion is given in Sec. 4.

2. Calculation methodology

We have studied the structural, electronic and magnetic properties of ZnS and ZnSe binary compounds, $Zn_{0.5}Cr_{0.5}S$ and $Zn_{0.5}Cr_{0.5}Se$ DMS alloys and $(ZnS)_2$/$Zn_{0.5}Cr_{0.5}Se$ and $(ZnSe)_2$/$Zn_{0.5}Cr_{0.5}S$ superlattices, using first-principle calculations based on the density functional theory (DFT) [46,47], namely the full potential linear muffin-tin orbital (FP-LMTO) method [48] with atomic plane-wave basis (PLW) representation [49]. These calculations are implemented in the computer code LmtArt. The Generalized Gradient Approximation (GGA) proposed by Perdew, Burke and Ernzerhof (PBE96) [50] is used to describe the energy for exchange and correlation term. In order to achieve energy eigenvalues convergence, the charge density and potential inside the MTSs are represented by spherical harmonics up to $I_{\max} = 6$. The self-consistent calculations are considered to be converged when the total energy of the system is stable at 10^{-6}Ry. The values of the sphere's radii (MTSs), the number of plane waves (NPLW), and the plane-wave cutoff (Ecut), used in our calculation, are summarized in Table I.

3. Results and discussion

3.1. Structural properties

The binary compounds ZnS and ZnSe belong to the II-VI family. They crystallize in the wurtzite-type (B4) structure, where zinc atoms occupy the position 2(b) with coordinates $1/3, 2/3, 0$ and $2/3, 1/3, 1/2$, and sulfur or selenium atoms are occupying the position 2(b) with coordinates $1/3, 2/3, u$ and $2/3, 1/3, u + 1/2$, where u is the dimensionless internal parameter that represents the distance between Zn plane and its nearest-neighbor S(Se) plane, in unit of c. $Zn_{0.5}Cr_{0.5}S$ and $Zn_{0.5}Cr_{0.5}Se$ DMS alloys were obtained by replacing one of the both Zn atoms constructing of wurtzite Zn(S,Se) with the transition metal Cr atom. Therefore, a Cr-doped model of $2 \times 2 \times 1$ supercell with 16 atoms was developed resulting from 50% Cr doping. DMS alloys crystallize in the same crystal structure as the "parent" compound, with a few exceptions. The magnetic ions were doped by substitution, occupying random lattice or sub-lattice positions in the host without forming a second phase. From the results and calculations built below, it is clear that the ZnS and ZnSe binary compounds, $Zn_{0.5}Cr_{0.5}S$ and $Zn_{0.5}Cr_{0.5}Se$ DMS alloys are suitable to form superlattices. In this work, superlattices are constituted by a sequence of alternating layers of binary compounds with DMS alloys respectively using a $2 \times 2 \times 2$ supercell model with 32 atoms (Fig. 1). Therefore, a periodic arrangement of quantum wells and barriers have consequently composed along the [001] growth axis direction. In order to determine the structural properties at equilibrium, in particular the parameter of the lattice constant a, the ratio

TABLE I. Parameters used in the calculations: number of plane wave (NPLW), energy cutoff (in Rydberg) and the muffin-tin radius (RMT in atomic units) for ZnS and ZnSe binary compounds, $Zn_{0.5}Cr_{0.5}S$ and $Zn_{0.5}Cr_{0.5}Se$ DMS alloys and $(ZnS)_2$/$Zn_{0.5}Cr_{0.5}Se$ and $(ZnSe)_2$/$Zn_{0.5}Cr_{0.5}S$ superlattices.

Compound	NPLW (Total)	Ecut(Ryd)	MTS (ua)			
			Zn	S	Se	Cr
ZnS	29156	214.0125	2.19	2.279	-	-
ZnSe	29156	193.1892	2.258	-	2.446	-
$Zn_{0.5}Cr_{0.5}S$	28796	223.5417	2.128	2.193	-	2.171
$Zn_{0.5}Cr_{0.5}Se$	28868	201.0925	2.195	-	2.356	2.241
$(ZnSe)_2$/$Zn_{0.5}Cr_{0.5}S$	59440	209.9332	2.196	2.294	2.358	2.263
$(ZnSe)_2$/$Zn_{0.5}Cr_{0.5}Se$	59416	209.4388	2.21	2.326	2.359	2.196

TABLE II. Calculated lattice constant a_0 (a.u), ratio c/a, internel parameter u, bulk modulus B (GPa), and pressure derivative of bulk modulus B' for ZnS and ZnSe binary compounds, $Zn_{0.5}Cr_{0.5}S$ and $Zn_{0.5}Cr_{0.5}Se$ DMS alloys and $(ZnS)_{0.5}/Zn_{0.5}Cr_{0.5}Se$ and $(ZnSe)_2/Zn_{0.5}Cr_{0.5}S$ superlattices.

compound	a_0 (a.u)	c/a	u	B (GPa)	B'
	7.291	1.649		119.9	
			0.375		
ZnS	7,214a	1,638a		74.0b	3.86406
			0.374c		
	7,353b	1,59b		76.4b	
	7.673	1.649			
			0.375		
ZnSe	7,542d	1,659d		101.5	3.99771
			0.371f		
	7,542e	1,659e			
	7.068	1.664			
$Zn_{0.5}Cr_{0.5}S$			0.374	130.8	3.65392
	7.206g	1.652g			
$Zn_{0.5}Cr_{0.5}Se$	7.465	1.662	0.376	123.4	3.0673
$(ZnSe)_{0.5}/Zn_{0.5}Cr_{0.5}S$	7.376	3.338	0.186	110.2	3.77696
$(ZnSe)_2/Zn_{0.5}Cr_{0.5}Se$	7.385	3.336	0.186	111.9	3.91693

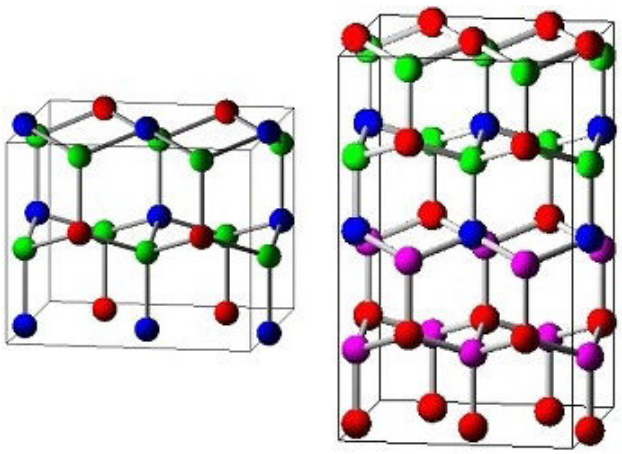

FIGURE 1. Crystal structure of wurtzite Cr-doped model of $2 \times 2 \times 1$ supercell with 16 atoms with 50% of Cr concentrations of DMS alloys, and the $2 \times 2 \times 2$ supercell model with 32 atoms of superlattices; Red is Zn, green is S, blue is Cr and magenta is Se.

c/a, and the internal parameter u, the compressibility modulus B and its first derivative B', we have carried out a self-consistent calculation of the total energy for the different variables of the wurteite structure. The results obtained were then interpolated or "fitted", using the Murnaghan equation of state [51]. The results of the calculation of the equilibrium structural parameters for the ZnS and ZnSe binary compounds, $Zn_{0.5}Cr_{0.5}S$ and $Zn_{0.5}Cr_{0.5}Se$ DMS alloys in the wurtzite structure are listed in Table II and compared to other experimental and theoretical [52-58] results. Our results are in accordance with those obtained theoretically and experimentally. We also notice that the parameters of the equilibrium increase from ZnS to ZnSe due to the small atomic radi of S compared to Se. For DMS, when the Zn atom is substituted by the Cr atom, which has an ionic radius less than that of Zn, the lattice constant decreases. Therefore, the compressibility modulus behaves the opposite of that of the lattice constants, while the internal parameter u changes randomly. According to the Table II analysis, we have noticed that the calculated equilibrium parameter a^0 of the both $(ZnS)_2/Zn_{0.5}Cr_{0.5}Se$ and $(ZnSe)_2/Zn_{0.5}Cr_{0.5}S$ superlattices are very close to $(a_{ZnS}+a_{ZnCrSe})/2$ and $(a_{ZnSe}+a_{ZnCrSs})/2$ respectively. This is explain by the fact that the atoms number in these directions (x axis) remains the same as bulk ZnS(Se) and ZnCrS(Se) for each layer respectively, and distributes identically in the both superlattices. For c/a ratio, and in both superlattices, it is found directly proportional to the number layers. This increase is principally because this direction is referring to the growth direction of our superlattices (z axis). We note that the (c/a) ratio follows the relationship $(c/a)_{ZnS}+(c/a)_{ZnCrSe}$ and $(c/a)_{ZnSe}+(c/a)_{ZnCrS}$ for both $(ZnS)_2/Zn_{0.5}Cr_{0.5}Se$ and $(ZnSe)_2/Zn_{0.5}Cr_{0.5}S$ superlattices, respectively. This proves the uniform direct proportionality between the number of layers and the mesh increase following the growth direction. The calculated equilibrium parameters of our superlattices agree with the linear relationship that linked the parameters in superlattice configurations [59]. For both superlattices, the compressibility modulus and the internal parameter u result to be equal to half of the sum of the values of their constitutive compounds.

3.2. Electronic properties

To reach a good comprehension of the electronic behavior, we calculated the electronic band structures along the high-symmetry directions of ZnS and ZnSe binary compounds, $Zn_{0.5}Cr_{0.5}S$ and $Zn_{0.5}Cr_{0.5}Se$ DMS alloys and

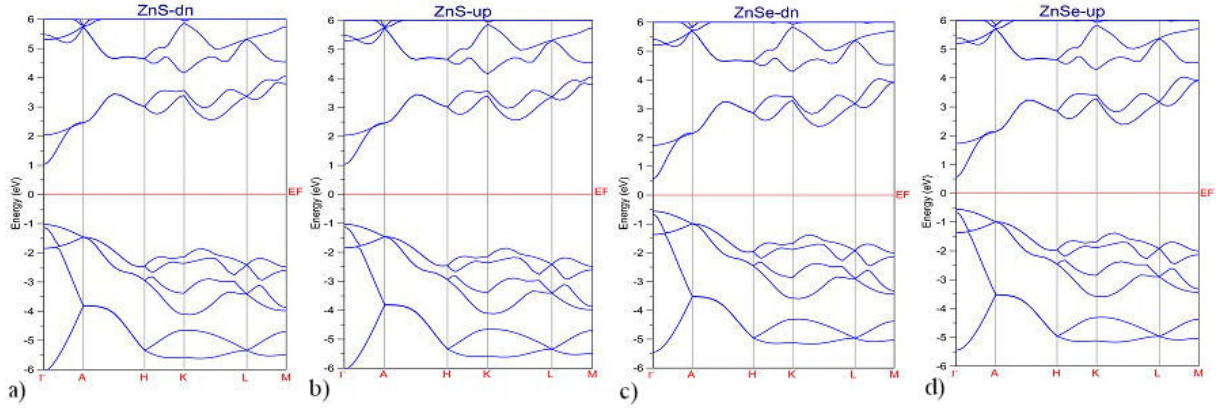

FIGURE 2. Band structures of majority spin [a), b)] and minority spin [c), d)] for ZnS and ZnSe binary compounds. The Fermi level is set to zero (horizontal line).

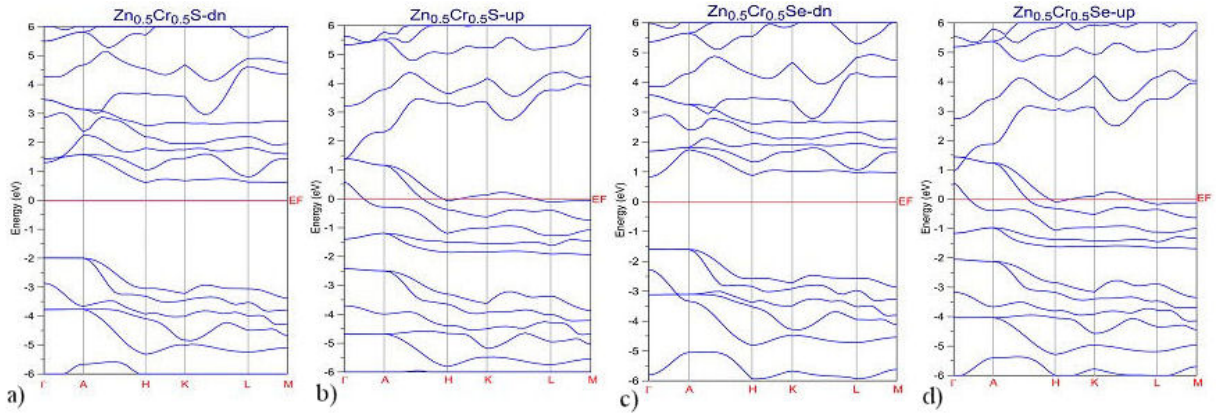

FIGURE 3. Spin-polarized band structures of majority spin [a), b)] and minority spin [c), d)] for $Zn_{0.5}Cr_{0.5}S$ and $Zn_{0.5}Cr_{0.5}Se$ DMS alloys. The Fermi level is set to zero (horizontal line).

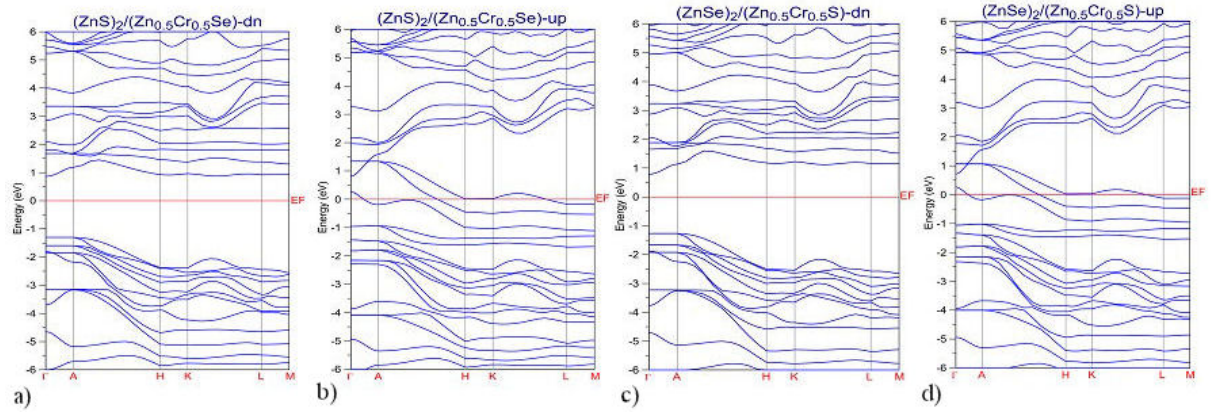

FIGURE 4. Spin-polarized band structures of majority spin [a), b)] and minority spin [c), d)] for $(ZnS)_2/Zn_{0.5}Cr_{0.5}Se$ and $(ZnSe)_2/Zn_{0.5}Cr_{0.5}S$ superlattices. The Fermi level is set to zero (horizontal line).

$(ZnS)_2/Zn_{0.5}Cr_{0.5}Se$ and $(ZnSe)_2/Zn_{0.5}Cr_{0.5}S$ superlattices at their equilibrium lattice constants. The obtained configurations are plotted in Figs. 2, 3 and 4, respectively. From Fig. 2, we notice that the majority and minority spins of ZnS and ZnSe have identical band structures characterized by a direct gap located at the Γ points of high symmetry ($E_{\Gamma-\Gamma}$). In addition, the symmetrical band structures indicate and confirm that ZnS and ZnSe compounds are not magnetic.

For $Zn_{0.5}Cr_{0.5}S$ and $Zn_{0.5}Cr_{0.5}Se$ DMS alloys and $(ZnS)_2/Zn_{0.5}Cr_{0.5}Se$ and $(ZnSe)_2/Zn_{0.5}Cr_{0.5}S$ superlattices, at first glance, we see that those figures clearly show the existence of a large exchange of splitting between the states of the majority spins (spin up) and the states of the minority spins (spin down) through the Fermi level. This means that the introduction of the transition metal atom Cr into the host semiconductor ZnS and ZnSe, leads to the appearance of a

TABLE III. Calculated nearby energy band edges E_c and E_v (eV), half-metallic ferromagnetic band gap E_g (eV) and their nature of minority-spin bands for ZnS and ZnSe binary compounds, $Zn_{0.5}Cr_{0.5}S$ and $Zn_{0.5}Cr_{0.5}Se$ DMS alloys and $(ZnS)_2/Zn_{0.5}Cr_{0.5}Se$ and $(ZnSe)_2/Zn_{0.5}Cr_{0.5}S$ superlattices.

compound	E_c (eV)	E_v (eV)	E_g (eV)	Nature
ZnS	1.031	-1.031	2.062	direct
ZnSe	-0.559	0.559	1.118	direct
$Zn_{0.5}Cr_{0.5}S$	-1.995	1.301	3.296	indirect
$Zn_{0.5}Cr_{0.5}Se$	-1.584	0.830	2.414	indirect
$(ZnSe)_2/Zn_{0.5}Cr_{0.5}S$	-1.267	0.790	2.057	direct
$(ZnSe)_2/Zn_{0.5}Cr_{0.5}Se$	-1.299	0.864	2.163	direct

magnetic order in all the compounds. Also, the main characteristics that present these figures are that the calculated spin-polarized band structures for all compounds exhibit a clearly half-metallic ferromagnetic (HMF) behavior. In addition, and as expected for $Zn_{0.5}Cr_{0.5}S$ and $Zn_{0.5}Cr_{0.5}Se$ DMS alloys and $(ZnS)_2/Zn_{0.5}Cr_{0.5}Se$ and $(ZnSe)_2/Zn_{0.5}Cr_{0.5}S$ superlattices, we notice that the band structures of the majority spins (spins up) exhibit a metallic behavior, while those of the minority spins (spins down) exhibit a clear half-metallic ferromagnetic gap denoted by EHMF. The values of the half-metallic ferromagnetic gaps obtained are reported in Table III. They represent the lowest energy difference between the minimum of the conduction band (CBM) and the maximum of the valence band (VBM). As it is well-known [60], PBE systematically underestimates band gaps. $Zn_{0.5}Cr_{0.5}S$ and $Zn_{0.5}Cr_{0.5}Se$ DMS alloys shows an indirect EHFM gap

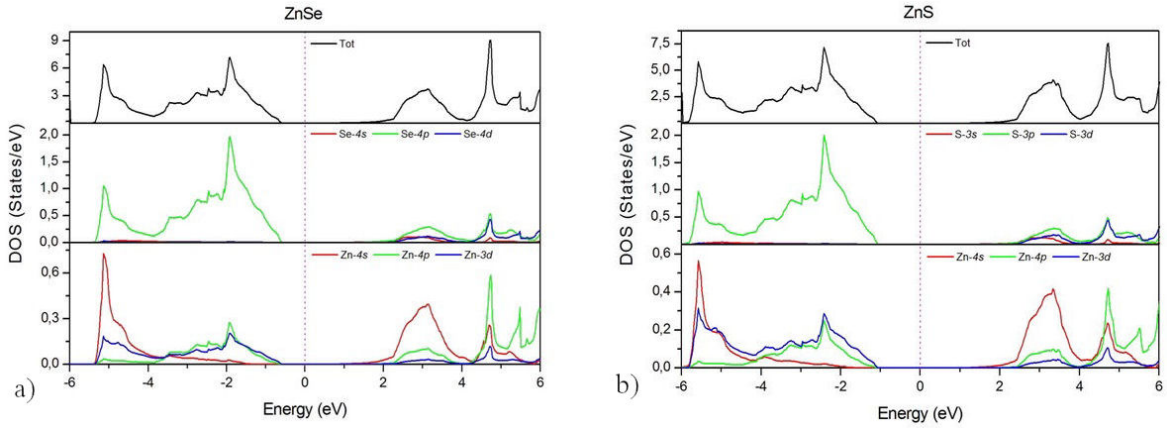

FIGURE 5. Total and partial DOS of ZnS and ZnSe binary compounds. The Fermi level is set to zero (vertical dotted line).

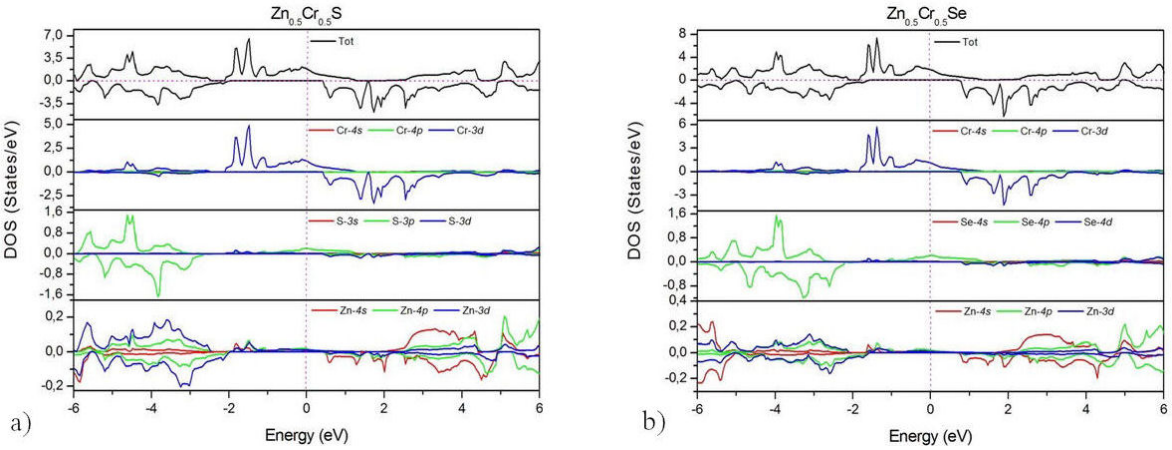

FIGURE 6. Spin-polarized total and partial DOS of $Zn_{0.5}Cr_{0.5}S$ and $Zn_{0.5}Cr_{0.5}Se$ DMS alloys. The Fermi level is set to zero (vertical dotted line).

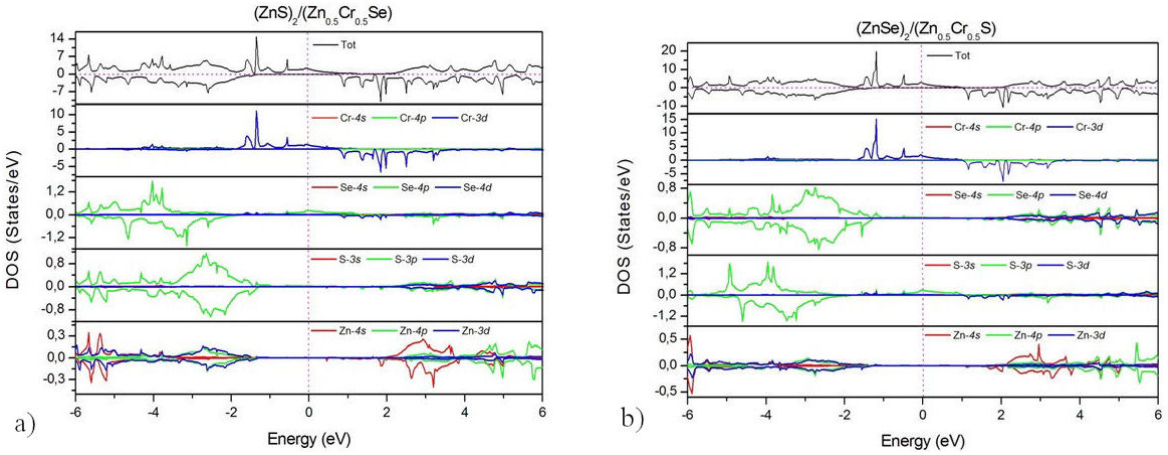

FIGURE 7. Spin-polarized total and partial DOS of $(ZnS)_{0.5}/Zn_{0.5}Cr_{0.5}Se$ and $(ZnSe)_2/Zn_{0.5}Cr_{0.5}S$ superlattices. The Fermi level is set to zero (vertical dotted line).

due to the fact that the CBM and the VBM are located, respectively, at Γ and R points. For $(ZnS)_2/Zn_{0.5}Cr_{0.5}Se$ and $(ZnSe)_2/Zn_{0.5}Cr_{0.5}S$ superlattices, the CBM and VBM are located at Γ point, which indicates the direct nature of the EHMF for these compounds.

To further clarify the electronic structure of ZnS and ZnSe binary compounds, $Zn_{0.5}Cr_{0.5}S$ and $Zn_{0.5}Cr_{0.5}Se$ DMS alloys and $(ZnS)_2/Zn_{0.5}Cr_{0.5}Se$ and $(ZnSe)_2/Zn_{0.5}Cr_{0.5}S$ superlattices, we have determined the total density of states (TDOS) and the corresponding partial or local densities (PDOS for partial density of states) which are shown in Figs. 5, 6 and 7, respectively. The positive values represent the states of the majority spins (spins up) and the negative values those of the minority spins (spins down). The Fermi level is located on the abscissa axis at zero and is represented by a vertical dots line.

Figure 6 clearly shows the existence of two distinct regions, separated by a band gap, one of which is located below the Fermi level E_F and the other in the valence band. The deepest region of the valence band is located in the energy interval from -6 eV to -4 eV and is dominated by the s-type states of Zn with a strong contribution from the p-type states of S(Se) and a small contribution of d-type states of Zn. The uppermost region of the valence band, located between -3 eV and E_F, consists mainly of the p states of S(Se) with a weak contribution from the p and d states of Zn. Concerning the conduction band, located above E_F, Fig. 5 shows that it is largely dominated by the s and p electronic states of Zn and the p and d states of S(Se). In the vicinity of Fermi level there is no DOS which confirm the semiconductor behavior of both ZnS and ZnSe.

The total densities of state (TDOS) of $Zn_{0.5}Cr_{0.5}S$ and $Zn_{0.5}Cr_{0.5}Se$ DMS alloys and $(ZnS)_2/Zn_{0.5}Cr_{0.5}Se$ and $(ZnSe)_2/Zn_{0.5}Cr_{0.5}S$ superlattices show a typical ferromagnetic half-metallic character due to the metallic behaviors of the majority spins and semiconductor of the minority spins thus leading to a full spin polarization of 100% at the Fermi level. These results are consistent with the band structures calculated and presented previously. The partial density of states (PDOS) shows that for both majority and minority spin chains of $Zn_{0.5}Cr_{0.5}S$ and $Zn_{0.5}Cr_{0.5}Se$ DMS alloys and $(ZnS)_2/Zn_{0.5}Cr_{0.5}Se$ and $(ZnSe)_2/Zn_{0.5}Cr_{0.5}S$ superlattices, the lower region of the valence band is dominated by the p states of S(Se) with a small contribution from the states d of Zn and a weak contribution of the p and s states of Zn and the d states of Cr while the upper region of the conduction band is formed by a minor contribution of the s and p states of Zn and S(Se). Moreover, the top of the valence band for the majority spins and the bottom of the conduction band for the minority spins come mainly from the 3d states of Cr. The upper regions of the valence bands of the majority spins for these compounds are mainly dominated by a strong hybridization between the p states of S(Se) and the 3d states of Cr giving them a metallic character. For minority spins, the 3d states of Cr disappear at the Fermi level leading to a typical semiconductor behavior.

3.3. Magnetic properties

The local structure around the Cr-impurity in the studied systems is a tetrahedral environment. The local structural distortions around the impurity and chemical disorder are expected to affect the obtained results for the energy gap and the local magnetic moments. In fact, if a Zn site is substituted by a Cr site, two of the six Cr valence electrons replace two Zn electrons. Of the other four electrons, two occupy the doubly degenerated e_g state, and two occupy the the triply degenerated t2g states. The triply degenerated states are filled up to two thirds. Consequently, the 3d(Cr) majority spin states cutting the Fermi level are partially filled, while the minority-spin states possess a large band gap at the Fermi level. So, the partially filled majority-spin t2g states suggest that the system is a half-metallic ferromagnet. Also, chromium impurity is responsible for narrowing the energy gap. In order to elucidate the origin of the magnetism in our compounds, we have reported in Table IV the total magnetic moments calculated

TABLE IV. Calculated total and local magnetic moments per Cr atom (in Bohr magneton μB) within the muffin-tin spheres and in the interstitial sites for $Zn_{0.5}Cr_{0.5}S$ and $Zn_{0.5}Cr_{0.5}Se$ DMS alloys and $(ZnS)_2/Zn_{0.5}Cr_{0.5}Se$ and $(ZnSe)_{0.5}/Zn_{0.5}Cr_{0.5}S$ superlattices.

Compound	Zn (μB)	S (μB)	Se (μB)	Cr (μB)	Int (μB)	Tot. (μB)
	0.04	-0.019	-	3.290	0.679	4.012
$Zn_{0.5}Cr_{0.5}S$	0.036	-	-0.073	3.425	0.622	4.018
$Zn_{0.5}Cr_{0.5}Se$	0.022	0.010	-0.061	3.354	0.657	4.012
$(ZnS)_2/Zn_{0.5}Cr_{0.5}Se$ $(ZnSe)_2/Zn_{0.5}Cr_{0.5}S$	0.016	-0.081	0.006	3.452	0.589	4.013

for $Zn_{0.5}Cr_{0.5}S$ and $Zn_{0.5}Cr_{0.5}Se$ DMS alloys and $(ZnS)_2/Zn_{0.5}Cr_{0.5}Se$ and $(ZnSe)_2/Zn_{0.5}Cr_{0.5}S$ superlattices, and the local magnetic moment in the muffin tin spheres Zn, S, Se and Cr atoms and in the interstitial sites. It is well known that a typical ferromagnetic half-metallic material should exhibit an integer value of the total magnetic moment. From the results in Table IV, we note that the values of the total magnetic moment for our compounds are closer than integer values, which indicate and confirm the ferromagnetic half-metallic nature of these compounds.

The 3d majority spins of Cr are partially occupied by four spin up electrons which create a magnetic moment of 4 μB per Cr atom. Moreover, it is noticed that the transition metal atom presents the main contribution to the total magnetic moment in the DMS and superlattices, while the initially non-magnetic Zn, S and Se atoms induce a minor contribution. Compared to the total magnetic moments predicted by Hund's rule for each compound, the local magnetic moment of Cr is reduced due to the strong p-d hybridization between the p orbitals of the host semiconductors and the 3d orbitals of magnetic impurity Cr. The p-d hybridization stabilizes the ferromagnetic ground state linked to double-exchange mechanism, and confirms that our compounds are predicted to be promising candidates for possible future semiconductor spintronic applications.

4. Conclusion

The manuscript work we conducted focused on the first-principle study of the structural, electronic and ferromagnetic half-metallic properties of ZnS and ZnSe binary compounds, $Zn_{0.5}Cr_{0.5}S$ and $Zn_{0.5}Cr_{0.5}Se$ DMS alloys and $(ZnS)_2/Zn_{0.5}Cr_{0.5}Se$ and $(ZnSe)_2/Zn_{0.5}Cr_{0.5}S$ superlattices in wurtzite-type structure.

- The study of the electronic structure through the band structures and the electronic densities of states reveals that $Zn_{0.5}Cr_{0.5}S$ and $Zn_{0.5}Cr_{0.5}Se$ DMS alloys and $(ZnS)_2/Zn_{0.5}Cr_{0.5}Se$ and $(ZnSe)_2/Zn_{0.5}Cr_{0.5}S$ superlattices are ferromagnetic half-metallics with a spin polarization of 100%.
- The main contribution in the magnetic moment is made by the transition metal atom in each compound and is reduced from the total value due to the strong hybridization between the 3d states of the transition metal atom (Cr) and the p states of the host bands.
- The p-d hybridization generates the antibonding states in the gap, which stabilize the ferromagnetic ground state linked to double-exchange mechanism, and confirms that our alloys are predicted to be promising candidates for possible future semiconductor spintronic applications.

1. M. Shur, Introduction to electronic devices (J. Wiley, 1996).
2. A. Bar-Lev, Semiconductors and electronic devices (Prentice-Hall, Inc., 1993).
3. P. Zhou *et al.*, Numerical modeling of magnetic devices, *IEEE Transactions on magnetics* **40** (2004) 1803, https://doi.org/10.1109/TMAG.2004.830511.
4. B. Bhushan, Tribology and mechanics of magnetic storage devices (Springer Science & Business Media, 2012).
5. S. D. Bader and S. S. P. Parkin, Spintronics, *Annu. Rev. Condens. Matter Phys.* **1** (2010) 71, https://doi.org/10.1146/annurev-conmatphys-070909-104123.
6. F. Pulizzi, Spintronics, *Nature materials* **11** (2012) 367, https://doi.org/10.1038/nmat3327.
7. M. Kaminska, A. Twardowski, D. Wasik, Mn and other magnetic impurities in GaN and other III-V semiconductors - perspective for spintronic applications, *J. Mater. Sci.: Mater. Electron.* **19** (2008) 828, https://doi.org/10.1007/s10854-007-9486-z.
8. H. Ohno, Properties of ferromagnetic III-V semiconductors, *J. Magn. Magn. Mater.* **200** (1999) 110, https://doi.org/10.1016/S0304-8853(99)00444-8.
9. B. Doumi, A. Mokaddem, F. Dahmane, A. Sayede, A. Tadjer, A novel theoretical design of electronic structure and half-metallic ferromagnetism in the 3d (V)-doped rock-salts SrS, SrSe, and SrTe for spintronics, *RSC Adv.* **112** (2015) 92328, https://doi.org/10.1039/C5RA16507E.
10. B. Doumi, A. Mokaddem, A. Sayede, F. Dahmane, Y.

Mogulkoc, A. Tadjer, First-principles investigations on ferromagnetic behaviour of $Be_{1-x}V_xZ$ (Z = S, Se and Te) (x = 0.25), *Superlattices Microstruct.* **88** (2015) 139, https://doi.org/10.1016/j.spmi.2015.09.008.

11. U. P. Verma, S. Sharma, N. Devi, P. S. Bisht, P. Rajaram, Spin-polarized structural, electronic and magnetic properties of diluted magnetic semiconductors $Cd_{1-x}Mn_xTe$ in zinc blende phase, *J. Magn. Magn. Mater.* **323** (2011) 394, https://doi.org/10.1016/j.jmmm.2010.09.016.

12. H. Ohno, Making nonmagnetic semiconductors ferromagnetic, *Science* **281** (1998) 951, https://doi.org/10.1126/science.281.5379.951.

13. G. A. Prinz, Magnetoelectronics, *Science* **282** (1998) 1660, https://doi.org/10.1126/science.282.5394.1660.

14. S. A. Wolf *et al.*, Spintronics: a spinbased electronics vision for the future, *Science* **294** (2001) 1488, https://doi.org/10.1126/science.1065389.

15. S. D. Sarma, Spintronics: A new class of device based on electron spin, rather than on charge, may yield the next generation of microelectronics, *Am. Sci.* **89** (2001) 516, http://www.jstor.org/stable/27857562.

16. S. J. Pearton *et al*., Advances in wide bandgap materials for semiconductor spintronics, Mater. Sci. Eng. R **40** (2003) 137, https://doi.org/10.1016/S0927-796X(02)00136-5.

17. I. Zutic, J. Fabian, S. D. Sarma, Spintronics: Fundamentals and applications, *Rev. Mod. Phys.* **76** (2004) 323, https://doi.org/10.1103/RevModPhys.76.323.

18. K. Sato, H. Katayama-Yoshida, Material Design of GaN-Based Ferromagnetic Diluted Magnetic Semiconductors, *Jpn. J. Appl. Phys.* **40** (2001) L485, https://doi.org/10.1143/JJAP.40.L485.

19. S. Y. Wu *et al.*, Synthesis, characterization, and modeling of high quality ferromagnetic Cr-doped AlN thin films, *Appl. Phys. Lett.* **82** (2003) 3047, https://doi.org/10.1063/1.1570521.

20. A. Mokaddem, B. Doumi, A. Sayede, D. Bensaid, A. Tadjer, M. Boutaleb, Investigations of Electronic Structure and Half-Metallic Ferromagnets in Cr- Doped Zinc-Blende BeS Semiconductor, *J. Supercond. Nov. Magn.* **28** (2015) 157, https://doi.org/10.1007/s10948-014-2828-1.

21. Y. Huang, W. Jie, G. Zha, First principle study on the electronic and magnetic properties in Zn0.75Cr0.25M (M = S, Se, Te) semiconductors, *J. Alloys Compd*. **539** (2012) 271, https://doi.org/10.1016/j.jallcom.2012.06.017.

22. H. Saito, V. Zayets, S. Yamataga, K. Ando, Magnetooptical studies of ferromagnetism in the II-VI diluted magnetic semiconductor Zn1-xCrxTe, *Phys. Rev. B* **66** (2002) 81201, https://doi.org/10.1103/PhysRevB.66.081201.

23. W. Mac, N. T. Khoi, A. Twardowski, M. Demianiuk, The s, p-d exchange interaction in Zn1-xCrxTe diluted magnetic semiconductors, *J. Cryst. Growth* **159** (1996) 993, https://doi.org/10.1016/0022-0248(95)00754-7.

24. M. Herbich, W. Mac, A. Twardowski, K. Ando, D. Scalbert, A. Petrou, The s,p-d exchange interaction of Cd0.997Cr0.003S, *J. Cryst. Growth* **184** (1998) 1000, https://doi.org/10.1016/S0022-0248(98)80209-1.

25. H. S. Saini, M. Singh, A. H. Reshak, M. K. Kashyap, Variation of half metallicity and magnetism of Cd1-xCrxZ (Z=S, Se and Te) DMS compounds on reducing dilute limit, *J. Magn. Magn. Mater.* **331** (2013) 1, https://doi.org/10.1016/j.jmmm.2012.10.044.

26. Y. Huang, W. Jie, G. Zha, First principle study on the electronic and magnetic properties in Zn0.75Cr0.25M (M = S, Se, Te) semiconductors, *J. Alloys Compd.* **539** (2012) 271, https://doi.org/10.1016/j.jallcom.2012.06.017.

27. M. Boucharef *et al*., First-principles study of the electronic and structural properties of (CdTe)n/(ZnTe)n superlattices, *Superlattices and Microstructures* **75** (2014) 818, https://doi.org/10.1016/j.spmi.2014.09.014.

28. L. Djoudi, M. Merabet, M. Boucharef, S. Benalia, and D. Rached, Firstprinciples calculations to investigate structural, electronic and optical properties of (BeTe)n/(CdS)n superlattices, *Superlattices and Microstructures* **75** (2014) 233, https://doi.org/10.1016/j.spmi.2014.07.029.

29. S. Benalia *et al*., Band gap behavior of scandium aluminum phosphide and scandium gallium phosphide ternary alloys and superlattices, *Materials Science in Semiconductor Processing* **31** (2015) 493, https://doi.org/10.1016/j.mssp.2014.12.021.

30. M. Asif Khan, A. B., J. N. Kuznia, and D. T. Olson, High electron mobility transistor based on a GaN-AlGaN heterojunction, *Applied Physics Letters* **63** (1993) 1214, https://doi.org/10.1063/1.109775.

31. S. Nakamura, M. Senoh, N. Iwasa, and S. Nagahama, High-brightness In- GaN blue, green and yellow light-emitting diodes with quantum well structures, *Japanese Journal of Applied Physics* **34** (1995) L797, https://doi.org/10.1143/JJAP.34.L797.

32. P. S. Zory., Quantum well lasers (Academic Press., 1993).

33. M. A. Haase, J. Qiu, J. M. DePuydt, and H. Cheng, Blue-green laser diodes, *Applied Physics Letters* **59** (1991) 1272, https://doi.org/10.1063/1.105472.

34. L. Freidman, Thermoelectric power of superlattices, *Surface science* **142** (1984) 241, https://doi.org/10.1016/0039-6028(84)90314-5.

35. H. Ohta, Y. Mune, K. Koumoto, T. Mizoguchi, Y. Ikuhara, Critical thickness for giant thermoelectric Seebeck coefficient of 2DEG confined in $SrTiO{-}3/SrTi_{0.8}Nb_{0.2}O_3$ superlattices, *Thin Solid Films* **516** (2008) 5916, https://doi.org/10.1016/j.tsf.2007.10.034.

36. S. K. Biswas, A. R. Ghatak, A. Neogi, A. Sharma, S. Bhattacharya, K. P. Ghatak, Simple theoretical analysis of the thermoelectric power in quantum dot superlattices of non-parabolic heavily doped semiconductors with graded interfaces under strong magnetic field, *Physica E* **36** (2007) 163, https://doi.org/10.1016/j.physe.2006.10.005.

37. X. Liu, A. Petrou, J. Warnock, B. T. Jonker, G. A. Prinz, and J. J. Krebs, Spin-dependent type-I, type-II behavior in a quantum well system, *Phys. Rev. Lett.* **63** (1989) 2280, https://doi.org/10.1103/PhysRevLett.63.2280.

38. M. von Ortenberg, Spin Superlattice with Tunable Minigap, *Phys. Rev. Lett.* **49** (1982) 1041, https://doi.org/10.1103/PhysRevLett.49.1041.

39. W. C. Chou, A. Petron, J. Warnock, and B. T. Jonker, Spin superlattice behavior in ZnSe/Zn0.99Fe0:0.01Se quantum wells, *Phys. Rev. Lett.* **67** (1991) 3820, https://doi.org/10.1103/PhysRevLett.67.3820.

40. N. Dai, H. Luo, F. C. Zhang, N. Samarth, M. Dobrowolska, and J. K. Furdyna, Spin superlattice formation in ZnSe/Zn1-xMnxSe multilayers, *Phys. Rev. Lett.* **67** (1991) 3824, https://doi.org/10.1103/PhysRevLett.67.3824.

41. B. T. Jonker *et al*., Spin separation in diluted magnetic semiconductor quantum well systems, *J. Appl. Phys.* **69** (1991) 6097, https://doi.org/10.1063/1.347779.

42. S. R. Jackson *et al*., Magnetooptical study of excitonic binding energies, band offsets, and the role of interface potentials in CdTe/Cd1-xMnxTe multiple quantum wells, *Phys. Rev. B* **50** (1994) 5392, https://doi.org/10.1103/PhysRevB.50.5392.

43. D. R. Yakovlev *et al*., Exciton magnetic polarons in short-period CdTe/Cd1-xMnxTe superlattices, *Phys. Rev. B* **52** (1995) 12033, https://doi.org/10.1103/PhysRevB.52.12033.

44. B. T. Jonker, H. Abad, L. P. Fu, W. Y. Yu, A. Petrou, and J. Warnock, Coexistence of Brillouin and Van Vleck spin exchange in Zn1Â¡xMnxSe/Zn1-yFeySe spin superlattice structures, *J. Appl. Phys.* **75** (1994) 5725, https://doi.org/10.1063/1.355595.

45. W. Ossau, B. Kuhn-Heinrich, G. Mackh, A. Waag, and G. Landwehr, Spin dependent confinement effects in $Cd_{0.9}Mn_{0.1}TeCd_{0.9}Mg_{0.1}Te$ spin superlattices, *J. Cryst. Growth* **159** (1996) 1052, https://doi.org/10.1016/0022-0248(95)00875-6.

46. P. Hohenberg, W. Kohn, Inhomogeneous Electron Gas, *Phys. Rev. B* **136** (1964) 864, https://doi.org/10.1103/PhysRev.136.B864.

47. W. Kohn, L. J. Sham, Self-Consistent Equations Including Exchange and Correlation Effects, *Phys. Rev. A* **140** (1965) 1133, https://doi.org/10.1103/PhysRev.140.A1133.

48. S. Yu. Savrasov, D. Yu. Savrasov, Full-potential linear-muffin-tin-orbital method for calculating total energies and forces, *Phys. Rev. B* **46** (1992) 12181, https://doi.org/10.1103/PhysRevB.46.12181.

49. S. Yu. Savrasov, Linear-response theory and lattice dynamics: A muffintin- orbital approach, *Phys. Rev. B* **54** (1996) 6470, https://doi.org/10.1103/PhysRevB.54.16470.

50. J. P. Perdew, K. Burke, and M. Ernzerhof, Generalized Gradient Approximation Made Simple, *Phys. Rev. Letts.* **77** (1996) 3865, https://doi.org/10.1103/PhysRevLett.77.3865.

51. F. D. Murnaghan, The Compressibility of Media under Extreme Pressures, *Proc. Natl. Acad. Sci. USA* **30** (1947) 244, https://doi.org/10.1073/pnas.30.9.244.

52. S. Desgreniers, L. Beaulieu, and I. Lepage, Pressure-induced structural changes in ZnS, *Phys. Rev. B* **61** (2000) 8726, https://doi.org/10.1103/PhysRevB.61.8726.

53. K. Wright, J. D. Gale, Interatomic potentials for the simulation of the zinc-blende and wurtzite forms of ZnS and CdS: Bulk structure, properties, and phase stability, *Phys. Rev. B* **70** (2004) 035211, https://doi.org/10.1103/PhysRevB.70.035211.

54. A. E. Merad, M. B. Kanoun, G. Merad, J. Cibert, and H. Aourag, Fullpotential investigation of the electronic and optical properties of stressed CdTe and ZnTe, *Mater. Chem. Phys.* **92** (2005) 333, https://doi.org/10.1016/j.matchemphys.2004.10.031.

55. M. Z. Huang and W. Y. Ching, Calculation of optical excitations in cubic semiconductors. I. Electronic structure and linear response, *Phys. Rev. B* **47** (1993) 9449, https://doi.org/10.1103/PhysRevB.47.9449.

56. S. J. Yun, G. Lee, J. S. Kim, S. K. Shin, and Y. G. Yoon, Electronic structure and optical absorption spectra of CdSe covered with ZnSe and ZnS epilayers, *Solid State Commun.* **137** (2006) 332, https://doi.org/10.1016/j.ssc.2005.10.029.

57. O. Zakharov, A. Rubio, X. Blase, M. L. Cohen, and S. G. Louie, Quasiparticle band structures of six II-VI compounds: ZnS, ZnSe, ZnTe, CdS, CdSe, and CdTe, *Phys. Rev. B* **50** (1994) 10780, https://doi.org/10.1103/PhysRevB.50.10780.

58. A. Lakdja, D. Mesri, H. Rozale, A. Chahed, and P. Ruterana, Spin polarization in wurtzite Zn1-xCrxS from first principles, *Phys. Status Solidi B* **249** (2012) 2222, https://doi.org/10.1002/pssb.201248266.

59. R. Belacel, S. Benalia, M. Merabet, L. Djoudi, and D. Rached, Theoretical study of structural, electronic and optical properties of ScxTl1-xP ternary alloys and (ScP)n/(TlP)n superlattices by FP-LMTO method, *Optik* **178** (2019) 243, https://doi.org/10.1016/j.ijleo.2018.09.093.

60. J. P. Perdew and M. Levy, Physical Content of the Exact Kohn-Sham Orbital Energies: Band Gaps and Derivative Discontinuities, *Phys. Rev. Lett.* **51** (1983) 1884, https://doi.org/10.1103/PhysRevLett.51.1884.